Principal Component Analysis under Population Genetic Models of Range Expansion and Admixture

Olivier Francois, Mathias Currat, Nicolas Ray, Eunjung Han, Laurent Excoffier, John Novembre

Preprint submitted to Molecular Biology and Evolution.
Manuscript ID MBE-09-0672 R

Title: Principal Component Analysis under Population Genetic Models of Range Expansion and Admixture

Authors: Olivier François[1*], Mathias Currat[2], Nicolas Ray[3,5], Eunjung Han[4], Laurent Excoffier[3,5], John Novembre[4]

Author affiliations:

1Laboratoire Techniques de l'Ingénierie Médicale et de la Complexité, Faculty of Medicine, University Joseph Fourier, Grenoble IT, Centre National de la Recherche Scientifique UMR5525, 38706 La Tronche, France.

2 Laboratory of Anthropology, Genetics and Peopling history (AGP), Department of Anthropology and Ecology, University of Geneva, 12 rue Gustave-Revilliod, 1227 Geneva, Switzerland.

3 Computational and Molecular Population Genetics lab, Institute of Ecology and Evolution, University of Berne, Baltzerstrasse 6, 3012 Berne, Switzerland.

4 Department of Ecology and Evolutionary Biology,University of California, Los Angeles, 621 Charles E. Young Dr South Box 951606 Los Angeles, CA 90095-1606, USA.

5 Swiss Institute of Bioinformatics, 1015, Switzerland.

***Corresponding author:** Olivier François , Laboratoire Techniques de l'Ingénierie Médicale et de la Complexité, Faculty of Medicine, University Joseph Fourier, Grenoble IT, Centre National de la Recherche Scientifique UMR5525, 38706 La Tronche, France.

Email: olivier.francois@imag.fr
Tel : +33 456 520 025

Abstract: In a series of highly influential publications, Cavalli-Sforza and colleagues used Principal Component (PC) analysis to produce maps depicting how human genetic diversity varies across geographic space. Within Europe, the first axis of variation (PC1) was interpreted as evidence for the demic diffusion model of agriculture, in which farmers expanded from the Near East ~10,000 years ago, and replaced the resident hunter-gatherer populations with little or no interbreeding. These interpretations of the PC maps have been recently questioned, as the original results can be reproduced under models of spatially co-varying allele frequencies without any expansion. Here, we study PC maps for data simulated under models of range expansion and admixture. Our simulations include a spatially realistic model of Neolithic farmer expansion and assume various levels of interbreeding between farmer and resident hunter-gatherer populations. An important result is that under a broad range of conditions the gradients in PC1 maps are oriented along a direction perpendicular to the axis of the expansion, rather than along the same axis as the expansion. We propose this surprising pattern is an outcome of the "allele surfing" phenomenon, which creates sectors of high allele frequency differentiation that align perpendicular to the direction of the expansion.

Introduction

Since its earliest uses (Cavalli-Sforza and Edwards 1963, Harpending and Jenkins 1973, Menozzi et al 1978), principal component analysis (PCA) has become a popular tool for exploring multi-locus population genetic data (Menozzi et al 1978; Rendine et al 1986; Cavalli-Sforza et al 1993; Cavalli-Sforza et al 1994; Patterson et al 2006; Novembre and Stephens 2008). PCA is a general method for representing high-dimensional data, for example individuals or populations, in a smaller number of dimensions. It has recently regained popularity as a tool to summarize large-scale genomic surveys, by providing covariates that might correct for population structure in genome-wide association studies (Price et al 2006; Patterson et al 2006), and by unveiling the main factors explaining the structure of genetic variation in large samples (Li et al 2008; Jakobsson et al 2008; Novembre et al 2008).

One way to explain PCA is as an algorithm that iteratively searches for orthogonal axes, described as linear combinations of multivariate observations, along which projected objects show the highest variance, and then returns the positions of objects along those axes (the principal components). For many data sets, the relative position of these objects (e.g. individuals) along the first few principal components provides a reasonable approximation of the covariance pattern among individuals in the larger data set. As a result, the first few PC values are often used to explore the structure of variation in the sample.

In one of the largest applications of PCA prior to the advent of large-scale single-nucleotide polymorphism (SNP) data, PCA was used to summarize allele-frequency data collected from worldwide populations of humans (Cavalli-Sforza et al 1994). The results of the PCA were visualized using “synthetic maps” or “PC maps” depicting how the principal component values for each sampled population vary across geographic space (with each principal component being displayed on a separate map). Notably, in many of the maps generated from their data, gradients and wave-like patterns were observed.

The interpretation of these gradient and wave-like patterns has been somewhat controversial (Sokal et al 1999, Novembre and Stephens 2008). In their original formulation, Cavalli-Sforza et al (1994) favored explanations in which the gradients and wave-like shapes were signatures of past expansion events. For example, Menozzi et al (1978) observed a large southeast (SE) to northwest (NW) gradient for PC1 across Europe and concluded that this gradient was the outcome of a SE to NW expansion of agriculturalist populations during the Neolithic era. In this *demic diffusion* model, farmers

expanded into Europe from the Near East ~10,000 years ago, replacing Paleolithic populations of hunter-gatherers with little or no admixture (Ammerman and Cavalli-Sforza 1984), (see also Davies 1998; Diamond and Bellwood 2003). The model implies that agriculture spread more by the migration of farming populations than by the cultural diffusion of the agricultural technologies.

One complication of this interpretation is that gradient and wave-like shapes arise quite generally in synthetic maps for data that are spatially structured (Novembre and Stephens 2008). In simple scenarios where samples are spaced evenly and covariance decays exponentially with distance, PC maps are expected to show regular patterns where typically the first map is of a gradient, the second is a gradient perpendicular to the first, and the third and fourth PC maps are “saddle” and “mound”-like wave shapes. Novembre and Stephens (2008) review mathematical arguments that explain these patterns and demonstrate their presence using simulations from simple population genetic models (symmetric migration between populations arranged on a square lattice and mutation-migration-drift equilibrium). Simulations in more complicated scenarios of spatial structure (unequal migration, irregular habitat shape, irregular sampling) evidenced distortions of these basic patterns, but the patterns generally included gradients and wave-like shapes. Thus, the observation of sinusoidal functions in PC maps, such as gradients or waves, is not strong evidence for specific past expansion events, because a large range of models inducing spatial structure will give rise to similar patterns.

An unanswered question is to what extent do sinusoidal patterns and gradients arise if a spatial expansion has occurred? Novembre and Stephens (2008) do not present simulations of range expansions, nor show for instance that observing a SE to NW gradient in PC1 is consistent or inconsistent with the Neolithic expansion. One might expect recent expansions will result in spatially structured data, and thus based on Novembre and Stephens’ results that some sinusoidal patterns should appear. However, if the patterns appear, is there a systematic distortion of the sinusoidal shapes as a signature of an expansion? For example, all else being equal, one might expect that the largest axis of genetic differentiation would be along the direction of the expansion, and thus if there is a gradient in PC1, its direction would be indicative of the direction of the historical expansion, as supposed in the classic interpretations of PC gradients.

Addressing these questions is particularly relevant to the contentious debate over the Neolithic expansion in Europe. While it is unlikely that lower PC-maps are indicative of unique historical expansions, the direction of the gradient in PC1 in the Menozzi et al analysis and in more recent analyses (Novembre et al 2008; Lao et al 2008; although see Heath et al 2009) might be consistent with a recent Neolithic expansion from the southeast towards the northwest.

To address the issue of how PCA behaves on samples of genetic variation obtained after range expansions, we explored a variety of spatial expansion scenarios using computer simulations to mimic massive migration from one or two sourcess. Previous simulations have been conducted by Rendine et al (1986), but due to computational advances, we are able to explore a wider range of scenarios. To specifically address the Neolithic expansion in Europe, we modeled an expansion using a spatial model of Europe, parameterized in such a way that migration rates vary according to topography and incorporating archaeological information about the timing of the arrival of modern humans in Europe as well as start of the Neolithic expansion. In order to get a broader perspective on the problem, we also explored a wide spectrum of other scenarios including more ancient expansions, multiple sources, and expansion on simple, regular lattices.

A surprising result of our simulation study is that the gradients observed in the first PC map often are found to be, contrary to most often formulated expectations, perpendicular to the main direction of expansion. We found this to be true for parameters representative of hypothesized Neolithic demic expansions into Europe from the Near-East. To explore the robustness of this result, we considered various introgression rates in our model of a European Neolithic expansion. We confirmed that the direction of greatest differentiation is perpendicular to the expansion by plotting how genetic differentiation increases with geographic distance along both geographic axes and by applying assignment methods. For example, when $K = 2$ we observed a gradient of assignment probabilities running perpendicular to the expansion. One possible mechanistic explanation for these results is that it is an outcome of the genetic surfing phenomenon (Edmonds et al 2004, Klopfstein et al 2006, Currat et al 2008). We discuss the implications of these findings for the analysis of population structure with PCA and assignment algorithms.

Material and Methods

Spatial Simulations. Spatial simulations of sampled molecular diversity were performed with a modified version of the computer program SPLATCHE, which uses a two-stage coalescent model of migration incorporating topographic information (Currat et al 2004). Forward in time, the demographic history of a population is simulated in a non-equilibrium stepping-stone model defined on a lattice of regularly spaced subpopulations or demes (Figure 1A). In this simulation, spatial information is encoded into a friction value for each deme (Figure 1B), and each deme sends migrants to its nearest neighbors at rate *m* with directional probabilities inversely proportional to the neighbors' friction values. Once a deme is colonized, its population size starts growing according to a standard logistic model with rate *r* and carrying capacity *C*. The model results in a wave-of-advance of the population, as shown in Figure 1C-D. The shape and speed of the wave-of-advance depend on the parameters of the model, *r, C, m*. Backward in time, the demographic parameters are used to generate gene genealogies for samples taken at different geographic locations under a coalescent framework. The population size *Ct*) of a given deme at any time *t* is used to compute the probability of coalescence for a pair of genes from that deme; backward migration probabilities are calculated using the number of migrants arriving from neighboring demes in the forward step. We used SPLATCHE to simulate various types of genetic markers including short tandem repeats (microsatellite data) and DNA sequence data.

Simulating Neolithic Expansion in Europe. Range expansion occurred in 64 by 42 lattices covering Europe from latitude 38ºN to 65ºN and from longitude 10ºW to 40ºE (2,688 cells, Figure 1B). In order to enable migration to and from the British Isles and Scandinavia, these regions were connected to the mainland by two narrow bridges associated with friction values ten-fold higher than in plains. The settlement of Europe was fixed at 1,600 generations before the present (Mellars 2006). Regarding this Paleolithic expansion, we used a simplified single-origin model, assuming that modern humans replaced archaic populations without genetic introgression as they arrived in Europe (Currat and Excoffier 2004). Technically, this expansion occurred on a first layer of demes representing hunter-gatherers. The carrying capacity of each deme in this first layer was set to $C = 50$, corresponding to a density of ~0.05 individual per km^2 (Steel et al 1998). The population size at the onset of the expansion was of 100 individuals (The "density overflow" option was used to spread the ancestral population over patches of up to ~20 demes). Four hundred generations before the present, a second range expansion started from the southeast (Anatolia). This occurred in a second layer of demes representing Neolithic farmer populations who could potentially interbreed with the resident populations. The carrying capacity of Neolithic demes and the size of the ancestral population were

set to values ten-fold larger than for hunter-gatherers (Ammerman and Cavalli-Sforza 1984). Hunter-gatherers ultimately disappear due to density-dependent competition with the farmers (see Currat and Excoffier (2005) for further details about the competition model used). Migration and growth rates have been calibrated to obtain a maximum of 500 generations for the duration of the Paleolithic settlement (Mellars 2004) and around 300 generations for the Neolithic transition (Pinhasi et al 2005). These scenarios correspond to the following values: migration rates m = 0.4, growth rates r = 0.5 (Paleolithic) or r = 0.4 (Neolithic). Two distinct sources for the Paleolithic expansion were considered: one in the Near-East, representing a hypothetical starting point for the arrival of modemore recently from in the center of the Iberian peninsula starting

Simulation on a Regular Lattice. Additional simulations of demic expansions without admixture were performed on the same lattice as for prehistoric scenarios, using a uniform friction map and sampling 10 individuals in every deme (26,880 individuals simulated for L = 100 unlinked loci). For these simpler simulations, we explored a wide range of demographic parameters. Expansions started from the southeast T = 500, T = 1000, or T = 2000 generations ago, migration rates took 3 distinct values m = 0.2, m = 0.5 and m = 0.8, growth rates took two values r = 0.5 and r = 1.0 and carrying capacities were set to either C = 500 or C = 1000, that were equal to the ancestral population size.

Principal Component Analysis and Assignment Algorithms. PCA was performed on a data set of multi-locus genotypes (individuals) to mimic the approaches used in the latest analyses of population genetic variation. The genotype matrix G was normalized by substracting the mean and dividing the resulting quantity by the standard deviation of the jth column (as in Patterson et al 2006; Novembre and Stephens 2008). Given the renormalized matrix, M, we computed the eigenvalues and eigenvectors of the sample covariance matrix, $X = MM'/n$, by applying the “prcomp” function of the R statistical package. Note that Menozzi *et al*'s original analyses applied PCA on a population level. For a fraction of the simulations performed here we used the population-based approach and we replicated our main results (results not shown). In addition to exploring the behavior of PCA on expansion simulations, we also applied Assignment Methods (AM) to each of the simulated scenarios. These methods are commonly used computational tools for inferring population genetic structure, and the connection between PCA and admixture estimation methods (which are closely related to assignment methods) has been recently investigated by Patterson et al (2006). In contrast to PCA, AM are model-based methods, which means that they use explicit model definitions for their likelihood function (Beaumont and Rannala 2004). AM programs use assignment of individuals to K putative populations also termed *genetic clusters*. The assignment of each individual genotype into each genetic cluster is carried out probabilistically by using Markov chain Monte Carlo methods. AM

analyses were carried out by using the computer programs STRUCTURE (Pritchard et al 2000) and TESS (Chen et al 2007; Durand et al 2009) under their default options. Although they used distinct prior distributions, these programs were grouped under a common terminology because their outputs displayed only minor differences for the data sets in our study.

Both the *k*th PC and membership probabilities in cluster *k* are vectors of length *n* with one entry for each individual. Each vector entry is associated with two geographic coordinates. To visualize how these vector values vary across geographical space, we performed spatial interpolation at a set of locations on a regular grid using the kriging method (exponential covariance model, Cressie et al 1993) and we displayed heat maps for the interpolated values of the PCs and assignment probabilities.

Results

We applied principal component analysis and assignment methods to simulated data sets generated under several demographic models of expansion of the Neolithic farmers in Europe. In these simulations we modeled demic or cultural diffusion of agriculture with and without admixture between early farmers and resident hunter-gatherers.

Demic Diffusion: Models Without Interbreeding. We began our study with spatial scenarios of Neolithic demic expansion in Europe in which there was no admixture between the expanding population and the resident population. Under these conditions, visual inspection of the results reveals that the PC1 maps exhibit continuous gradients for a large majority of the simulated datasets. Remarkably, in 19 of the 20 simulations that ended with 100% of Neolithic ancestry in the European gene pool (full replacement), the gradients are oriented along an axis that starts from the southwest and ends to the northeast of Europe (SW-NE axis, Figure 2A and pattern 1 in Table 1). This axis is perpendicular to the direction of expansion that runs along a southeast to northwest axis. In order to see if this unexpected result was due to the contours of the European continent, we simulated expansions from the southwest of Europe (source in the center of Spain). We chose southwest Europe not because it is a likely origin for the settlement of Europe, but to see how in simulations, the origin of an expansion affects resultant PCA patterns. In this case, we find NW to SE gradients in the PC1 map, which are again perpendicular to the main direction of the expansion (SW to NE, 10 out of 10 simulations, Figure 2C). For both sources of expansion, PC2 maps generally highlight the regions of Scandinavia (Figure 2A and 1C) and PC3 the British Isles, which presumably reflects their

geographic isolation in our simulated habitat (see below for further discussion).

When we ran the assignment methods for K = 2 clusters, the resulting assignment probability maps show patterns that are strongly similar to those observed in PC1 maps, with membership probability in one of the two clusters decreasing along a SW-NE axis (Figure S1 AB). AM maps for K = 3 clusters exhibit features similar to the PC1 and PC2 maps, showing one cluster either in Scandinavia or in the British Isles and two other partitioning the European mainland along the SW-NE axis (Figure S1 CD).

One concern might be that the unexpected result is influenced by the specific set of 60 sampling locations or by the habitat shape and friction surfaces used for the simulations. To investigate this possibility, we ran additional simulations on a lattice of the same size as implemented in our spatial simulations for expansions starting from the south-east but with uniform migration rates and regular sampling across space. In addition, we sampled the complete set of 2,688 demes, with 10 individuals per deme. For a majority of the tested combinations of the model parameters, the first PC separates southwestern populations from northeastern ones. Again, this direction is perpendicular to the main axis of expansion. An example of this typical pattern is shown in Figure 2B, for $m = 0.2$, $r = 0.5$, $C = 100$ and $T = 1{,}000$ (C is the carrying capacity of each deme, T is the number of generation since the onset of the expansion). In all the 36 simulations, PC2 showed a gradient running in the direction orthogonal to that apparent in the PC1 map. The pattern visible in PC1 consistently changed over all replicates from a SW-NE to an EW gradient when T increased, and the gradients in the maps of PC1 and PC2 become weaker and eventually non-existent as genetic variation homogenizes across the habitat with time (example replicates shown in Figure S2). For example, this happens when the age of the expansion is set to T = 1,000 generations, and when the migration rate is simultaneously increased to m = 0.5 implying that Cm was greater than 50 (Figure S2). For the lowest values of T, m, and C (T = 500, m = 0.2, C = 100) we find that the direction of the PC1 gradient is variable from replicate to replicate – aligning with the expansion ~50% of the time. This phenomenon is reminiscent of variation in the direction of PC1 observed amongst replicate simulations from equilibrium stepping-stone models in which there is no directional spatial pattern in the data (see Figure S1 of Novembre and Stephens 2008), and was not observed after restoring the European habitat shape for the same demographic parameters or after increasing the carrying capacities to C = 500.

For these simulations, we also simulated sequence data sets consisting of 2,000 loci of 200 bp each. The mutation rate, equal to 10^{-7} per bp per generation, is a comparable rate of novel mutant alleles as having a more realistic mutation rate of 10^{-8} per bp distributed in 2,000 non-recombining sequences of 2Kb. We measured the extent of isolation-by-distance for: $m=0.2$, $r=0.5$, $C=100$ and $T=1{,}000$.

Isolation-by-distance was assessed by regressing the logarithm of genetic distances (measured as $F_{ST}/(1-F_{ST})$) between pairs of samples on the logarithm of their geographic distances (Slatkin 1993), where F_{ST} was obtained according to the definition of Hudson et al (1992). Figure 3 provides evidence that genetic distances increased significantly faster with geographic distances along the transect perpendicular to the expansion than along the direction of the expansion ($P < 10^{-9}$).

Admixture Models: Interbreeding with Paleolithic Residents. We next examined what would happen if there was any interbreeding between an expanding Neolithic population from the southeast with a resident Paleolithic population. To this aim, we reproduced the framework and the choice of parameters of Currat and Excoffier (2005) to simulate the genetic impact of the Neolithic transition. Briefly, a first expansion started around 1,500 generations ago from the Near East on a first layer of demes representing Paleolithic hunter-gatherer populations and covering all Europe. We specified levels of local gene flow between the resident and the invading populations so that the Paleolithic genes represented ~20%, 80% or more than 90% of the current European gene pool. These proportions were computed by the program SPLATCHE at each sampling location, and then averaged over the sampling area. In ~77.5% (31 out of 40) of the simulations ending with 20% or 80% of Paleolithic ancestry, we observe patterns similar to those obtained under a pure Neolithic demic diffusion model (Table 1 and Figure 4A). In other words, PC1 exhibits a gradient along the SW-NE axis which runs perpendicular to the Neolithic expansion axis. As previous simulations have revealed the existence of gradients of admixture along the Neolithic expansion axis (Currat and Excoffier 2005), we computed maps of the fraction of Neolithic ancestry in current populations (Figure 5). These maps represent the local proportions of Neolithic genes in the European genetic pool. In the examples with 20% and 80% of final Paleolithic ancestry, we obtain a gradient of introgression along the direction of Neolithic expansion (Figure 5 for the case of a final Paleolithic contribution equal to 80%). Thus this pattern can occur at the same time as a PC gradient is running perpendicular to the same axis. We also observed a similar behavior for genetic diversity, computed as the (average) variance in microsatellite allele size, which displays a gradient running along the recent expansion axis (Figure S3). In conclusion, if the proportion of ancient lineages in the current genetic pool is not very high (< 80%), the direction of PC1 gradient is found to be perpendicular to the most recent (Neolithic) expansion.

When the local levels of interbreeding are higher than γ ~ 6% - 7% we get two categories of patterns that depend on where the Paleolithic expansion took place: 1) Assuming a Paleolithic expansion that starts from the SW at the onset of the Last Glacial Maximum (~20,000 years ago) and a Neolithic expansion that starts from the SE, the gradients in the PC1 map align with the main direction of

Neolithic expansion (SE-NW axis, Table 1 and Figure 4C); 2) When both the ancient and the recent expansions start from the SE (arrival of modern humans followed by the Neolithics), then the direction of PC1 gradients is along the East-West axis in most simulations (9 out of 10 simulations, Table 1 and Figure 4B). For these simulations with proportions of Paleolithic ancestry in current genomes ancestry reaching values ~90%, the patterns of genetic variation in the current populations are more influenced by the Paleolithic population and where it expanded from than by Neolithic movements. In agreement with this, in cases where the Paleolithic expansion is from the SE, the PC gradients along the EW axis are similar to those obtained under an ancient expansion from the SE (Figure S4). Likewise, the gradients of genetic diversity do not run parallel to the direction of the most recent expansion, but in the direction of the most ancient one (Figure S3).

Discussion

Gradients in PC1 are Often Perpendicular to the Main Direction of Expansion. In our computer simulations of the colonization of Europe by southeastern populations of early farmers, we observe gradients in PC1 maps in agreement with a spatial structuring of genetic variation across the continent. An important and striking result is that, when the local rates of admixture between Neolithic colonists and Paleolithic residents are low, these gradients are consistently oriented in a direction perpendicular to the axis of the Neolithic expansion, rather than along the same axis as the expansion. Another important result is that when the final genetic pool is highly introgressed by the ancient (Paleolithic) population (> 80% introgression), we found the PC1 gradient to be perpendicular to the direction of the Paleolithic expansion, and as a result can in some cases be parallel to the direction of the most recent (Neolithic) expansion. For example, if there has been an ancient expansion from a southwestern refugium and the level of Neolithic ancestry in the current gene pool is less than 20%, our results show that PC1 evidence a SE to NW gradient.

To confirm these results, we ran simulations of expansions in a homogeneous environment, and found PC1 maps again showed a gradient running perpendicular to the expansion front, just as in simulations including realistic environmental features. The results suggest that PC1-map patterns are due to the process of expansion, rather than being an artifact of the geographical constraints we simulated. Assignment programs with $K = 2$ clusters also inferred gradients of probability that run perpendicular to the expansion axis, validating the PC1 gradient as an important axis of differentiation. Finally, by measuring the extent of genetic differentiation as function of distance, we

found a stronger extent of genetic differentiation on an axis perpendicular rather than along the expansion axis. It thus seems that a gradient perpendicular to the expansion is not an artifact of a given method, but that it rather reflects a true main underlying axis of differentiation among the populations. The question arises as to why differentiation would be perpendicular to the direction of expansion.

The Surfing Phenomenon. One possible explanation for the direction of the gradients we observed is the *allele surfing phenomenon* (Edmonds et al 2004; Klopfstein et al 2006; Excoffier and Ray 2008). In the surfing phenomenon, the repeated founder effects that occur at the edge of an expansion wave create conditions for low-frequency alleles to "surf" to higher frequencies and even to fixation at the wave-front. As the wave moves forward, large patches of habitat become colonized with the "surfing" allele and form "sectors" of low genetic diversity at a given locus (Hallatschek et al 2007). These sectors are often fixed for an allele that has low frequency elsewhere in the habitat; leading to strong differentiation between sectors (Hallatschek et al 2007; 2008). Because these sectors are aligned along the direction of expansion – there is actually the potential for substantial differentiation *perpendicular* to the axis of expansion (as illustrated in Figure 6; see also Excoffier and Ray 2008).

Common Allele Frequency Distributions. To investigate whether common alleles show patterns consistent with surfing, we examined a particular data set from our geographic simulations (1,200 individuals, 60 samples, no interbreeding). In these simulations, we generated sequence data (400 Kb per individual distributed evenly over 2,000 independent loci, mutation rate = 10^{-7} per bp per generation). For these data we obtained 10,581 segregating sites with a frequency spectrum highly skewed towards low-frequency alleles (Figure 7A). The high frequency of singletons (approximately 80%) indicates a strong departure from the constant-size neutral frequency spectrum, for which the expected value is around $0.14 \sim (\sum_1^{600} 1/i)^{-1}$. When PC1 was computed from the loci with minimum allele frequency (MAF) > 10, the synthetic map was not different from the result obtained with all the data, although these high frequency mutations occurs only at a small fraction of the polymorphic sites (108 sites; Figure 7B-C). In contrast, when PC1 was computed from the sites with MAF less than 10, a strikingly distinct picture emerged, displaying an optimum at the center of the area (Figure 7D). This suggests that the PC1 gradient is driven strongly by the geographic distribution of the common alleles, many of which are likely to have become common due to allele surfing (Currat and Excoffier 2005; Excoffier and Ray 2008). To study the common alleles in more detail, we generated allele frequency maps for the most common mutations (MAF > 30). We found that their spatial distributions exhibit regions where one allele was nearly absent and others where the same allele was completely fixed (Figure S5). These regions have approximately conic shapes, and they approximate the

"sectors" described by Hallatschek et al. In geographically explicit simulations, sectors of high frequencies were also observed in areas accessible only through the narrow bridges in Scandinavia and in the British Isles, where spatial bottlenecks might have reinforced genetic drift.

How Likely is Allele Surfing to be a Determinant of Genetic Structure? The question arises of whether allele surfing is an exceptional phenomenon that only occurs due to our specific simulated parameter values or if it is expected to play a role in real populations. The probability of surfing alleles depends on many factors, including the amount of local diversity (Edmonds et al 2004), the demographic parameters (Klopfstein et al 2006), potential admixture with resident populations during the expansion phase (Currat et al 2008), and geographical heterogeneity (Burton and Travis 2008). For conditions approximating a mutation rate of 10^{-8} per bp per generation, we find that about one mutation per 100Kb has a chance to reach a final frequency over 20% (Figure 7A). Although these surfing mutations represent less than 1% of the total number of all mutations, this small fraction of high frequency mutations seems to dominate the variability represented by PC1. Although a rare phenomenon in our simulations, surfing indeed deeply influences the patterns uncovered in PC or AM maps. In addition, as surfing is not restricted to mutations arising during the expansion phase, rare alleles present in the gene pool of the expanding population and those introduced via introgression also have the possibility to produce surfing patterns. Further, as the size of the population at the source of the expansion is rather small (C = 100 for the hunter-gatherers and C = 1,000 for the farmers), most mutations have occurred during or after the expansion in our simulations, while a large fraction of the mutations present in current European populations originated in Africa and were therefore already present in the populations having initially colonized Europe. It follows that the surfing of standing variants has probably been underestimated in our simulations.

Effects of Geographic Constraints. When a realistic geography of Europe is taken into account in the simulation, PC maps often reveal strong differentiation at the edge of the range of the expansion, typically in Scandinavia, or less frequently in the British Isles and in the Iberian peninsula. The very common Scandinavian cluster does not persist when geographic constraints are removed and when simulations are performed into a uniform environment. Clusters arising at the edge of the continental area might be interpretable as a combination of the effects of isolation-by-distance and the effects of geographic bottlenecks, like land-bridges across seas or corridors in mountain ranges (Burton and Travis 2008). The narrow land bridge we have introduced to connect the south of Sweden to Denmark is likely to lead to increased genetic drift and founder effects, and thus to differentiation between populations on opposite sides of the Baltic Sea. Note that the Scandinavian and the British

populations were also identified in separate clusters by the AM programs. A second point is that we do not expect our results to hold in long, rectangular (approximately one dimensional) habitats. Indeed, in expansions into linear habitats the wave-front is necessarily very narrow, and it will be difficult for sectors to form, and so alleles that surf will likely not be distributed in patches perpendicular to the axis expansion.

Criticisms of the simulation model. Although our simulation model realistically accounts for contours and geographic barriers in Europe, it is not meant to be a very detailed model of European prehistory. First of all, there is unavoidable uncertainty about the parameters used for characterizing population densities, rates of expansion and rates of migration (see Rowley-Conwy 2009). Events that occurred at small geographic scales, like fluctuations in carrying capacities due to variation in resource availability or due to local changes in the environment are ignored. Thus, it is possible that the model fails to reproduce every particular aspect of local genetic diversity. However the simulation model is still useful for giving interesting insights as it captures large-scale temporal and spatial aspects of European prehistory, including, for example, the timing of the spread of agriculture, the relative densities of hunter-gatherer and farmer populations, and admixture between hunter-gatherer and farmer populations. Previous work has shown how expansions with admixture produce clines in the proportion of Neolithic ancestry that sensibly follow the direction of expansion (Currat and Excoffier 2005), and we show here how diversity decreases as one moves along the direction of the expansion. Both of these patterns are expected in expansion models, and they suggest that the simulations, which also reproduce observed patterns (Chiaroni et al 2009), are meaningful. In this framework, the PC maps described in this study are robustly observed under a wide range of model parameters.

Implications for the Interpretation of Human Genetic Variation in European Populations.
For some time, population geneticists have been attempting to reconstruct the ancient demographic history of the Europeans and it has been the source of considerable debate (e.g. Barbujani and Goldstein 2005, Jobling et al 2004). Major ancestral processes that have been suggested are an initial Paleolithic colonization, later re-expansions from southern refugia, the Neolithic dispersal of early farmers, or trans-Mediterranean gene flow. The relative importance of these events for explaining standing patterns of genetic variation is however difficult to assess from archaeological data. As a result, a variety of genetic data sets and analysis methods have been used to study this problem. Our goal here has been to clarify how to best interpret results produced by PCA analysis, one particular exploratory tool used in this long debate**.** We found that at odds with conventional wisdom, the gradient in PC1 can orient perpendicular to the direction of an expansion under a wide range of

conditions. It thus appears that NW/SE gradients previously observed in PC1 plots of Europe are inconsistent with many simple models of Paleolithic or Neolithic expansions from the Near-east. The simulation results might suggest a role of expansions from soutwestern refugia after the last glacial maximum. However Heath et al (2008) found PC1 to align with an E/W gradient in Europe, Lao et al (2008) found a PC1 gradient that ran N/S, NW/SE gradients were observed by Menozzi et al (1978) and by Cavalli-Sforza et al (1994), and a NNW/SSE gradient was observed by Novembre et al (2008). The direction of PC gradients is difficult to interpret due to the influence of the sampling scheme (Novembre and Stephens 2008, McVean 2009). Because of these uncertainties, we withhold making conclusions and suggest that future progress will occur by more directly looking at spatial patterns of variation in Europe (such as potential sector patterns) in place of methods such as PCA.

The simulation study we conducted here gives two general insights about spatial patterns of variation that might be observed under models of population expansions: 1) Spatial patterns of genetic variation (gradients / clines) can arise under a broad range of expansion scenarios, just as they do in equilibrium isolation-by-distance models. 2) There can be substantial differentiation along an axis perpendicular to the direction of an expansion, presumably due to allele surfing. Many studies have shown that gradients in variation exist across Europe (Menozzi et al 1978, Sokal and Menozzi 1982, Sokal et al 1989, Chikhi et al 1998, Rosser et al 2000, Barbujani and Pilastro 1992, Chikhi et al 2002, Dupanloup et al 2004); most recently finding that such gradients even exist at spatial scales on the order of 100 of kilometers (Bauchet et al 2007; Tian et al 2008; Lao et al 2008, Novembre et al 2008, Heath et al 2008, Sabatti et al 2009, Price et al 2009).

Evidence for the directionality of spatial patterns is more difficult to summarize as substantial differences exist across studies and one needs to be specific about exactly what aspect of variation is being observed. Using directional correlograms, Sokal et al (1989) show many loci consistent with NW/SE clines (particularly HLA loci), but other loci show evidence for other directional clines. Inferences of the proportion of Neolithic ancestry have shown both patterns that decay with distance from the Near East using Y-chromosome markers (Chikhi et al 2002) as well as East-West patterns using 8 loci (Dupanloup et al 2004). The recent availability of large-scale SNP data helps alleviate concerns about making inferences from a small number of loci and promises to reveal more consistent genome-wide patterns. In this vein, two more recent large-scale SNP-based studies (Lao et al 2008, Auton et al 2009) have both observed a gradient in levels of haplotype diversity and linkage disequilibrium that are roughly north-south and with high levels of diversity in the Italian and Iberian peninsulas. Notably, these patterns seem unexpected under a demic diffusion model from the Near East and are more consistent with an impact of trans-Mediterranean gene flow (Auton et al

2009), larger population sizes in the southwest (Lao et al 2008) or with hypotheses of southern glacial refugia. However, the analysis of high-throughput SNP data from European populations is still in an exploratory phase. Further work, for instance looking specifically for patterns of variation consistent with "sectors" generated by surfing alleles, will likely shed more light on the genetic history of European populations. As always, the results will need to be integrated with other approaches, and an additional promising avenue of work is ancient DNA analyses. Comparing mitochondrial DNA sequences from 20 hunter-gatherer skeletons with those from modern Europeans, Bramanti et al (2009) found that most of the ancient hunter-gatherers in central Europe share haplotypes that are rare in Europeans today, perhaps pointing towards a highly dynamic history of human population movements in Europe.

Conclusions. A previous study showed that the original patterns observed in PCA might not reflect any expansion events (Novembre and Stephens 2008). Here we find that under very general conditions, the pattern of molecular diversity produced by an expansion may be different than what was expected in the literature. In particular, we find conditions where an expansion of Neolithic farmers from the southeast produces a greatest axis of differentiation running from the southwest to the northeast. This surprising result is seemingly due to allele surfing leading to sectors that create differentiation perpendicular to the expansion axis. While a lot of our results can be explained by the surfing phenomenon, some interesting questions remain open. For example the phase transition observed for relatively small admixture rates between Paleothic resident and Neolithic migrant populations occurs at a value that is dependent on our simulation settings, and further investigations would be needed to better characterize this critical value as a function of all the model parameters. Another unsolved question is to know why the patterns generally observed in PC2 maps for our simulations settings sometimes arise in PC1 maps instead. These unexplained examples remind us that PCA is summarizing patterns of variation in the sample due to multiple factors (ancestral expansions and admixture, on-going limited migration, habitat boundary effects, and the spatial distribution of samples). In complex models such as our expansion models with admixture in Europe, it may be difficult to tease apart what processes give rise to any particular PCA pattern. Our study emphasizes that PC (and AM) should be viewed as tools for exploring the data, but that the reverse process of interpreting PC and AM maps in terms of past routes of migration remains a complicated exercise. Additional analyses – with more explicit demographic models - are more than ever essential to discriminate between multiple explanations available for the patterns observed in PC and AP maps. We speculate that methods exploiting the signature of alleles that have undergone surfing may be a powerful approach to study range expansions.

Acknowledgements

NR and LE were partially supported by Swiss NSF grants No. 3100A0-112072 and 3100A-126074 to LE. MC was supported by Swiss NSF grant No 3100A0-112651 to Alicia Sanchez-Mazas whom we thanks for her support. OF was partially supported by a French ANR grant BLAN06-3146282 MAEV, and he thanks the IXXI Institute of Complex Systems. JN was supported by the Searle Scholar program. JN and EH were supported by NSF grant 0733033.

Cited Literature

1. Ammerman AJ, Cavalli-Sforza LL (1984) *The Neolithic Transition and the Genetics of Populations in Europe.* Princeton University Press, Princeton.

2. Auton A, Bryc K, Boyko AR, Lohmueller KE, Novembre J et al (2009) Global distribution of genomic diversity underscores rich complex history of continental human populations. Genome Research 19:795-803.

3. Barbujani GG, Pilastro A (1993) Genetic evidence on origin and dispersal of human populations speaking languages of the Nostratic macrofamily. Proceedings of the National Academy of Sciences USA 90:4670-4673.

4. Barbujani G, Sokal RR, Oden NL (1995) Indo-European origins: a computer-simulation test of five hypotheses. American Journal of Physical Anthropology **96**:109-132.

5. Barbujani GG, Bertorelle G, Chikhi L (1998) Evidence for paleolithic and neolithic gene flow in Europe. Am J Hum Genet 62:488–491.

6. Barbujani GG, Goldstein DB (2004) Africans and Asians abroad: Genetic diversity in Europe. *Annual Review of Genomics and Human Genetics* 5:119-150.

7. Bauchet M, McEvoy B, Pearson LN, Quillen EE, Sarkisian T, Hovhannesyan K, Deka R, Bradley DG, Shriver MD (2007) Measuring European population stratification with microarray genotype data. Am J Hum Genet 80:948-56.

8. Beaumont MA, Rannala B (2004) The Bayesian revolution in genetics. Nat Rev Genet 5: 251-261.

9. Bramanti B, Thomas MG, Haak W, Unterlaender M, Jores P et al (2009) Genetic discontinuity between local hunter-gatherers and central Europe's first farmers Science 26(5949):137-40.

10. Belle EMS, Landry P-A, Barbujani G (2006) Origins and evolution of the Europeans' genome: Evidence from multiple microsatellite loci. Proc R Soc B 273:1595-1602.

11. Burton OJ, Travis JM (2008) Landscape structure and boundary effects determine the fate of mutations occurring during range expansions. Heredity 101(4):329-40.

12. Cavalli-Sforza LL, Edwards AWF (1963) Analysis of human evolution. In Genetics Today: Proceedings of the 11th International Congress of Genetics, The Hague, The Netherlands, S.J. Geerts, ed. New York: Pergamon, no. 3, 923-993.

13. Cavalli-Sforza LL, Menozzi P, Piazza A (1993) Demic expansions and human evolution. Science 259: 639–646.

14. Cavalli-Sforza LL, Menozzi P, Piazza A (1994) *The History and Geography of Human Genes*. Princeton University Press, Princeton.

15. Chiaroni J, Underhill PA, Cavalli-Sforza LL (2009) Y chromosome diversity, human expansion, drift, and cultural evolution. *Proc Natl Acad Sci U S A* 106:20174-20179.

16. Chikhi L, Destro-Bisol G, Bertorelle G, Pascali V, Barbujani G (1998) Clines of nuclear DNA markers suggest a recent Neolithic ancestry of the European gene pool. Proc Natl Acad Sci USA 95: 9053–9058.

17. Chikhi L, Nichols RA, Barbujani G, Beaumont MA (2002) Y genetic data support the Neolithic demic diffusion model. Proc Natl Acad Sci USA 99:11008–11013.

18. Chen C, Durand E, Forbes F, François O (2007) Bayesian clustering algorithms ascertaining spatial population structure: A new computer program and a comparison study. Mol Ecol Notes 7:747–756.

19. Cressie NAC (1993) *Statistics for Spatial Data.* Wiley New-York.

20. Currat M, Excoffier L (2004) Modern humans did not admix with Neanderthals during their range expansion into Europe. PLoS Biol 2: 2264-2274.

21. Currat M, Ray N, Excoffier L (2004) SPLATCHE: a program to simulate genetic diversity taking into account environmental heterogeneity. Mol Ecol Notes 4(1): 139-142.

22. Currat M, Excoffier L (2005) The effect of the Neolithic expansion on European molecular diversity. Proc R Soc B 272: 679–688.

23. Currat M, Ruedi M, Petit RJ, Excoffier L (2008) The hidden side of invasions: massive introgression by local genes. Evolution 62:1908-1920.

24. Davies N (1998) *Europe: a History*. Harper Perennial, New York.

25. Diamond J, Bellwood P (2003) Farmers and their languages: The first expansions. Science 300:597-603.

26. Dupanloup I, Bertorelle G, Chikhi L, Barbujani G (2004) Estimating the impact of prehistoric admixture on the genome of Europeans. Mol Biol Evol 21: 1361-72.

27. Durand E, Jay F, Gaggiotti OE, François O (2009) Spatial inference of admixture proportions and secondary contact zones. Mol Biol Evol 26: 1963-1973.

28. Edmonds CA, Lillie AS, Cavalli-Sforza LL (2004) Mutations arising in the wave front of an expanding population. Proc Natl Acad Sci USA 101: 975-979.

29. Excoffier L, Ray N (2008) Surfing during population expansions promotes genetic revolutions and structuration. Trends Ecol Evol 23: 347-351.

30. Haak W, Forster P, Bramanti B, Matsumura S, Brandt G, et al (2005) Ancient DNA from the First European Farmers in 7500-Year-Old Neolithic Sites. *Science:* 310: 1016-1018.

31. Hallatschek O, Hersen P, Ramanathan S, Nelson DR (2007) Genetic drift at expanding frontiers promotes gene segregation. Proc Natl Acad Sci USA 104:19926-19930.

32. Hallatschek O, Nelson DR (2008) Gene surfing in expanding populations. Theor Popul Biol 73:158-170.

33. Harpending HC, Jenkins T (1973) Genetic distance among southern African populations, in *Method and Theory in Anthropological Genetics*, edited by M. Crawford and P. Workman, Albuquerque: University of New Mexico Press.

34. Heath SC, Gut IG, Brennan P, McKay JD, Bencko V et al (2008) Investigation of the fine structure of European populations with applications to disease association studies. Eur J Hum Genet 16:1413–1429.

35. Hudson, R.R., Slatkin, M. and Maddison W.P. 1992. Estimation of levels of gene flow from DNA sequence data. Genetics, 132(2):583–589.

36. Jakobsson M, Scholz SW, Scheet P, Gibbs JR, VanLiere JM et al (2008) Genotype, haplotype and copy-number variation in worldwide human populations. Nature 451:998-1003.

37. Jobling MA, Hurles ME, Tyler-Smith C (2004) *Human Evolutionary Genetics: origins, peoples and disease*. London/New York: Garland Science Publishing.

38. Klopfstein S, Currat M, Excoffier L (2006) The fate of mutations surfing on the wave of a range expansion. Mol Biol Evol 23: 482-490.

39. Lao O, Lu TT, Nothnagel M, Junge O, Freitag-Wolf S et al (2008) Correlation between genetic and geographic structure in Europe. Curr Biol 18:1241–1248.

40. Li JZ, Abscher DM, Tang H, Southwick AM, Casto AM et al (2008) Worldwide human relationships inferred from genome-wide patterns of variation. Science 319:1100-04.

41. McVean G (2009) A genealogical interpretation of principal components analysis. PLoS Genet 5(10): e1000686. doi:10.1371/journal.pgen.1000686

42. Mellars P (2004) Neanderthals and the modern human colonization of Europe. Nature 432: 461-465.

43. Mellars P (2006) Archeology and the dispersal of modern Humans in Europe: Deconstructing the "Aurignacian". Evol Anthropol 15:167-182.

44. Menozzi P, Piazza A, Cavalli-Sforza L (1978) Synthetic maps of human gene frequencies in Europeans. Science 201:786–792.

45. Novembre J, Stephens M (2008) Interpreting principal components analyses of spatial population genetic variation. Nat Genet 40:646-649.

46. Novembre J, Johnson T, Bryc K, Kutalik Z, Boyko AR, Auton A, Indap A, King KS, Bergman S, Nelson MR, Stephens M, Bustamante CD (2008) Genes mirror geography within Europe. Nature 456: 98-101.

47. Patterson NJ, Price AL, Reich D (2006) Population structure and eigenanalysis. PLoS Genet 2: e190.

48. Pinhasi R, Fort J, Ammerman AJ (2005) Tracing the origin and spread of agriculture in Europe. PLoS Biol 3: e410.

49. Price AL, Patterson NJ, Plenge RM, Weinblatt ME, Shadick NA, Reich D (2006) Principal components analysis corrects for stratification in genome-wide association studies. Nat Genet 8:904-90.

50. Price AL, Helgason A, Palsson S, Stefansson H, St. Clair D, et al. 2009 The impact of divergence time on the nature of population structure: An example from Iceland. PLoS Genet 5(6): e1000505.

51. Pritchard JK, Stephens M, Donnelly P (2000) Inference of population structure using multilocus genotype data. Genetics 155:945–959

52. Rendine S, Piazza A, Cavalli-Sforza LL (1986) Simulation and separation by principal components of multiple demic expansions in Europe. Am Nat 128, 681–706.

53. Richards M, Côrte-Real H, Forster P, Macaulay V, Wilkinson-Herbots H et al (1996) Paleolithic and Neolithic lineages in the European mitochondrial gene pool. Am J Hum Genet 59:185–203.

54. Rosser ZH, Zerjal T, Hurles ME, Adojaan M, Alavantic D et al (2000) Y-chromosomal diversity in Europe is clinal and influenced primarily by geography, rather than by language. Am. J. Hum. Genet. 67:1526-1543.

55. Rowley-Conwy P (2009) Human prehistory: Hunting for the earliest farmers. Current Biology 19: R948-R949.

56. Sabatti C, Service SK, Hartikainen AL, Pouta A, Ripatti S et al (2009) Genome-wide association analysis of metabolic traits in a birth cohort from a founder population. Nat. Genet. 41: 35-46.

57. Seldin MF, Shigeta R, Villoslada P, Selmi C, Tuomilehto J, Silva G, Belmont JW, Klareskog L, Gregersen PK (2006) European population substructure: clustering of northern and southern populations. PLoS Genet (2):e143.

58. Semino O et al (2000) The genetic legacy of Paleolithic Homo sapiens in extant Europeans: a Y chromosome perspective. Science 290: 1155–1159.

59. Slatkin M (1993) Isolation-by-distance in equilibrium and non-equilibrium populations. Evolution 47:264-279.

60. Sokal RR, Menozzi P (1982) Spatial autocorrelation of HLA frequencies in Europe support demic diffusion of early farmers. Am. Nat. 119:1-17.

61. Sokal RR, Harding RM, Oden NL (1989) Spatial patterns of human gene frequencies in Europe. Am J Phys Anthropol 80:267–294.

62. Sokal RR, Oden NL, Wilson C (1991) New genetic evidence for the spread of agriculture in

Europe by demic diffusion. Nature 351:143–145

63. Sokal RR, Oden NL, Thomson BA (1999) A problem with synthetic maps. Hum Biol 71, 1–13

64. Steele J, Adams JM, Sluckin T (1998) Modeling Paleoindian dispersals. World Archaeology 30: 286-305.

65. Tian C, Plenge RM, Ransom M, Lee A, Villoslada P, et al. (2008) Analysis and Application of European Genetic Substructure Using 300 K SNP Information. PLoS Genet 4: e4.

66. Torroni A, Bandelt H-J, D'Urbano L, Lahermo P, Moral P, Sellitto D, Rengo C, Forster P, Savantaus M-L, Bonné-Tamir B, Scozzari R (1998) MtDNA analysis reveals a major late Paleolithic population expansion from southwestern to northeastern Europe. Am J Hum Genet 62:1137-1152.

Figures and Tables

Figure 1. Illustration of the simulated demographic processes. A) A schematic representation of how Europe is modeled as an irregular array of demes. To simulate genetic data, multilocus genotypes are sampled at uniformly distributed locations, taking 20 individuals at each sampling site (crosses). B) The friction map that encodes the inverse migration rates used in the demographic simulations. Dark values indicate low migration rates. C-D) Picture of the wave-of-advance model at a fixed simulation time. Range expansion starts from the bottom-right corner of the area. Demes with the light grey colors are saturated at their carrying capacities (white demes are empty), while the dark grey colors indicate lower densities in particular at the front of the expansion.

Figure 2. PC1 and PC2 maps. A) Data set simulated under a spatially realistic scenario of demic diffusion of Neolithic farmers in Europe without interbreeding with Paleolithic residents (100% of Neolithic ancestry in current genomes). B) Range expansion on a regular lattice starting from the bottom-right corner. Ten individuals are sampled in each of the 64 x 42 demes. The average values of the first two eigenvectors are displayed for each deme. C) Data set simulated under a scenario of an

hypothetic demic expansion originating in the center of the Iberian peninsula. Time of origin T = 400 generations ago, migration rate m = 0.5, growth rate r = 0.5, carrying capacity N = 500, no admixture with resident populations.The arrows indicate the origin of the expansion.

Figure 3. Isolation by distance. Regression of genetic distance, computed as $F_{ST}/(1-F_{ST})$, on the logarithm of geographic distance for a simulation of range expansion on a regular lattice (start from the bottom-right corner, no admixture). Dashed line: demes in the direction of expansion (main diagonal of the habitat). Solid line: demes in the direction perpendicular to expansion (second diagonal).

Figure 4. The three main patterns observed in PC1 maps under spatially realistic models of the demic expansion of Neolithic farmers in Europe with admixture with resident hunter-gatherer populations. A) Simulations with more than 20% of Neolithic ancestry in current genomes (Paleolithic expansions starting either from the SE or from the SW). B) Simulations with less than 20% of Neolithic ancestry in current genomes (Paleolithic expansion from the south east). C) Simulations with less than 20% of Neolithic ancestry in current genomes (Paleolithic expansion from the south west). The black arrows indicate the origin of the Neolithic expansion, and the white arrows indicate the origin of the Paleolithic expansion.

Figure 5. Proportions of Neolithic ancestry in current genomes. Simulation with 20% of Neolithic average contribution. Similar maps were obtained regardless of the Paleolithic origin of the residents.

Figure 6. Recurrent founder effects during range expansions create sectors where one allele is completely fixed while the same allele is absent elsewhere. These regions have approximately conic shapes, and they increase genetic differentiation along the axis perpendicular to the direction of expansion.

Figure 7. Common alleles carry out population structure. Sequence data including 2,000 unlinked sequences of length 200 bp simulated under a regular lattice (1,200 individuals, 60 samples, mutation rate = 10^{-7}/bp/gen). A) Folded frequency spectrum computed from more than 10,000 polymorphic sites. B) PC1 map for all polymorphic sites. C) PC1 map for sites with MAF<10. D) PC1 map for sites with MAF>10.

Supplementary Figure Legends

Figure S1. Comparison of maps obtained after applying the assignment method implemented in the clustering program TESS and to those obtained from PCA to a particular scenario of demic diffusion of Neolithic farmers without contact with Paleolithic residents in Europe (same as in Figure 1). A) PC1 map. B) Map of assignment probabilities to cluster 1 for K = 2. C) PC2 map. D) Map of assignment probabilities to cluster to 2 for K = 3. Similar results for B) and D) where obtained with STRUCTURE. The ordering of the clusters is arbitrary.

Figure S2. PC1 maps for simulations of a range expansion on a regular lattice, with an expansion originating in the bottom-right corner). Ten individuals are sampled in each of the 64 x 42 demes. The average values of the first two eigenvectors are displayed for each deme.

Figure S3. Heat maps for the genetic diversity computed as the variance in the number of microsatellite repeats. A) and B) Models with low (or no) admixture with hunter-gatherers originating from the southwest (Iberian peninsula). The gradient of genetic diversity is parallel to the direction of the Neolithic expansion, and it is orthogonal to the first PC gradient. C) and D) Models with relatively high levels of admixture with hunter-gatherers originating from the southwest (Iberian peninsula). The gradient of genetic diversity is parallel to the direction of the Paleolithic expansion, and still orthogonal to the first PC gradient.

Figure S4. Synthetic maps (PC1 and PC2) for a data set simulated under a hypothetic scenario of an expansion originating in Anatolia in ancient times (time of origin T = 1,500 ago, migration rate m = 0.4, growth rate r = 0.5, carrying capacity N = 50).

Figure S5. Heat map for the frequency of two common alleles. A) and C). Sectors with high frequency in eastern Europe. Minor allele frequency increases with distance to the Iberian peninsula. B) and D) Sectors in Central Europe.

Paleolithic expansions from the South-East				
	Pattern 1 (SW-NE gradient)	Pattern 2 (W-E gradient)	Pattern 3 (SE-NW gradient)	Other patterns
Final levels of Neolithic ancestry				
100%	**9/10**	1/10		
80%	**8/10**			2/10
20%	**9/10**	1/10		
10%	1/10	**9/10**		
Paleolithic expansions from the South-West				
	Pattern 1 (SW-NE gradient)	Pattern 2 (W-E gradient)	Pattern 3 (SE-NW gradient)	Other patterns
Final levels of Neolithic ancestry				
100%	**10/10**			
80%	**7/10**	1/10		2/10
20%	**7/10**	2/10		1/10
10%			**10/10**	

Table 1. Frequency of observed patterns in PC1 maps for simulations of Neolithic range expansions from the south-east (80 replicates). The top panel of results is for the case where Paleolithic expansions were modeled from the south-east and the bottom panel for the case with expansions from the south-west. The first row within each panel (100% Neolithic ancestry) corresponds to a demic Neolithic expansions without admixture with resident paleolithic populations. Subsequent rows (<100% final Neolithic ancestry) are for Neolithic expansions in which there was admixture with resident Paleolithic populations. Pattern 1 displays a SW-NE gradient. Pattern 2 displays an east-west gradient. Pattern 3 exhibits a gradient from the SE to the NW. A summary of the 3 patterns can be found in Figure 3. The other patterns observed in PC1 represents clusters in Scandinavia or in the British Isles

A

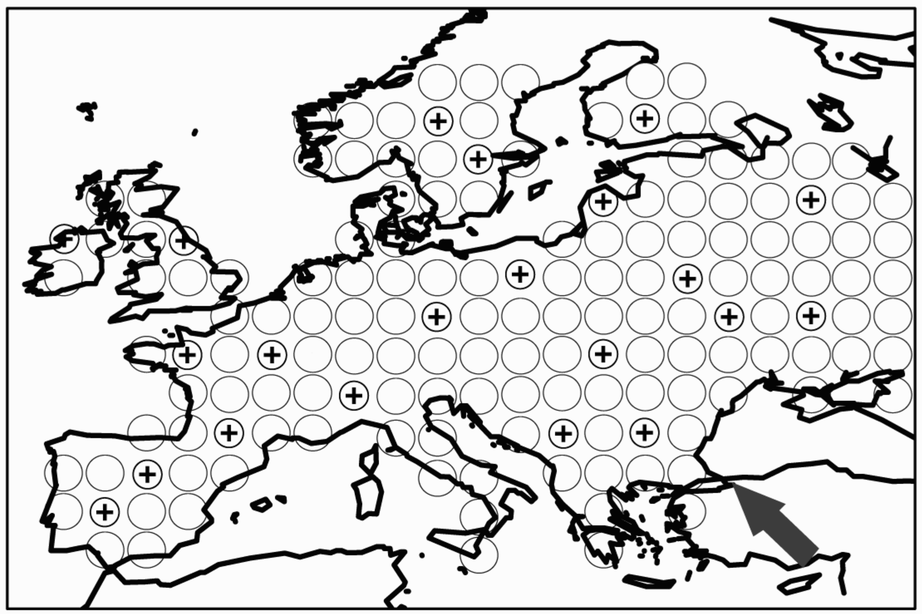

B

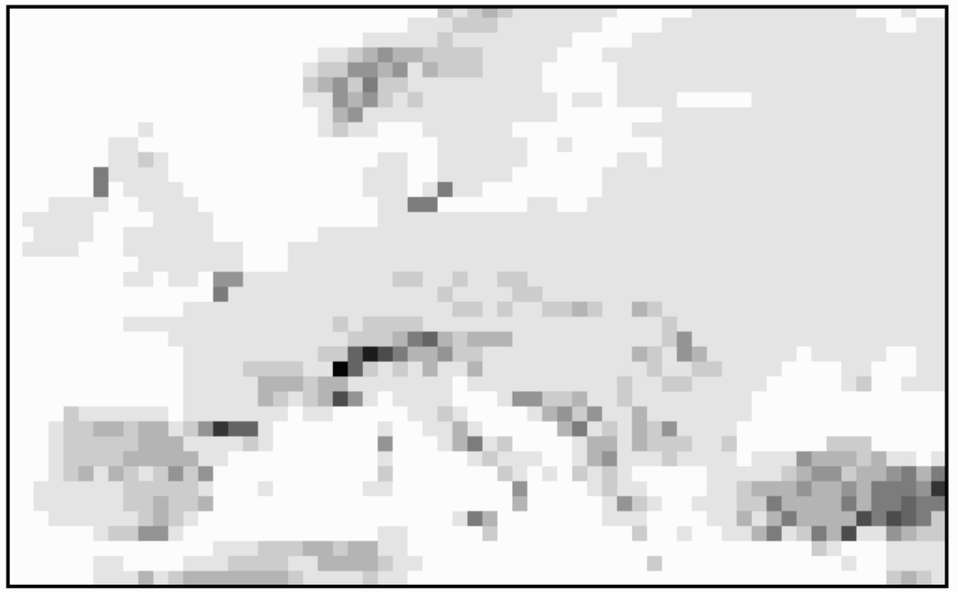

C

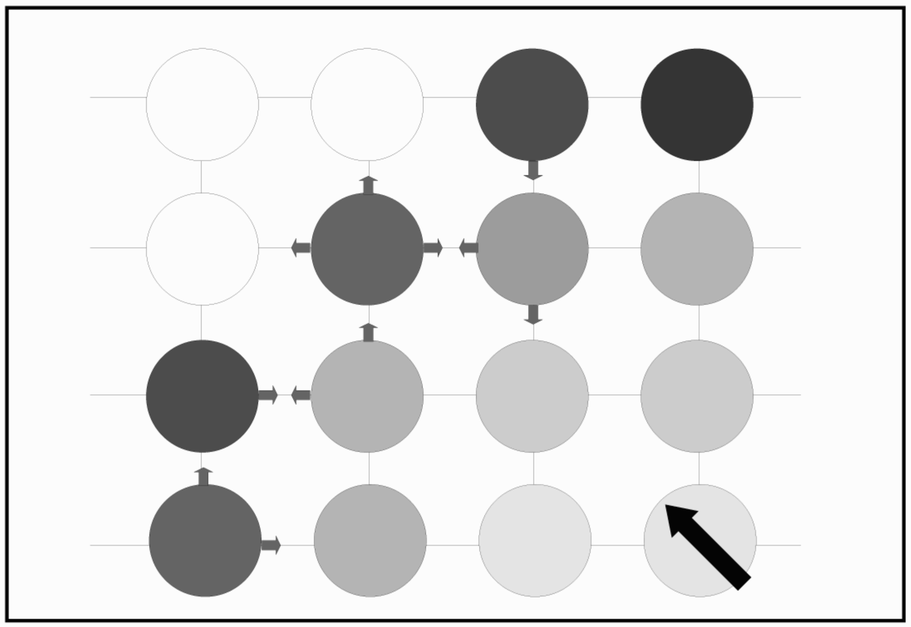

D

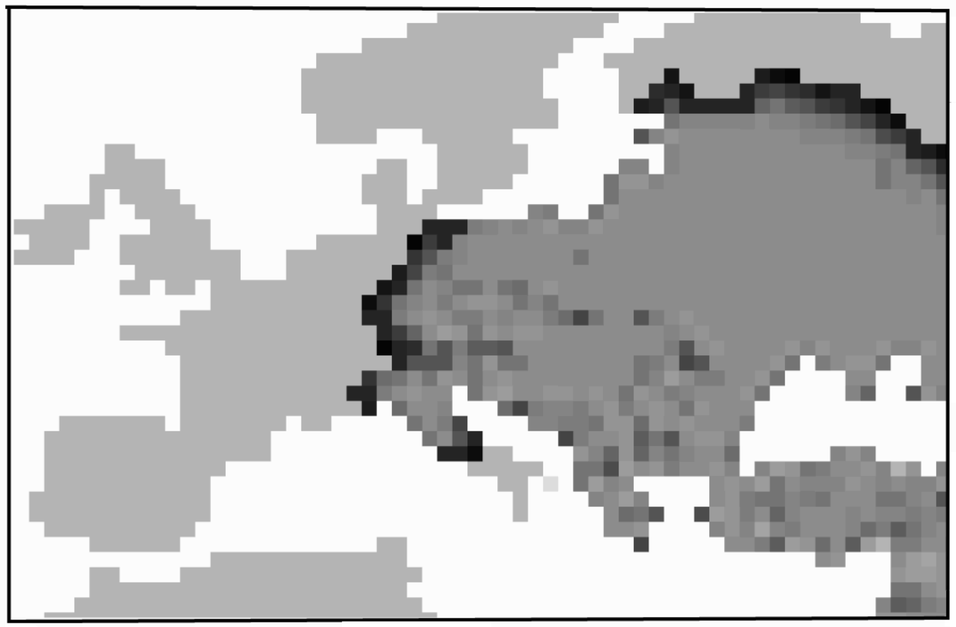

PC1

PC2

A

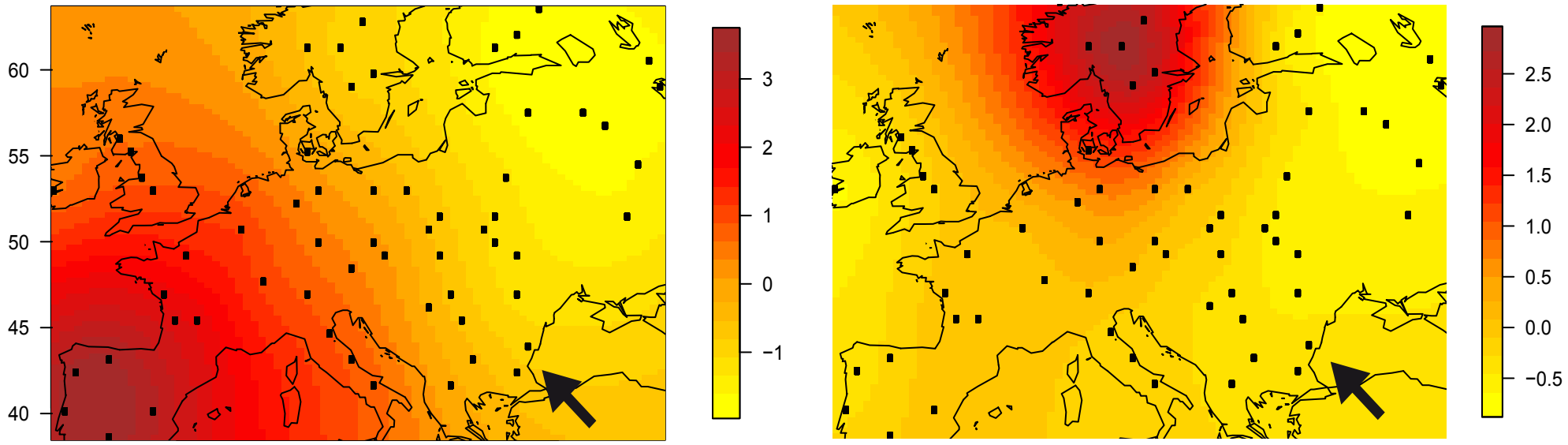
60
55
50
45
40
3
2
1
0
−1
2.5
2.0
1.5
1.0
0.5
0.0
−0.5

B

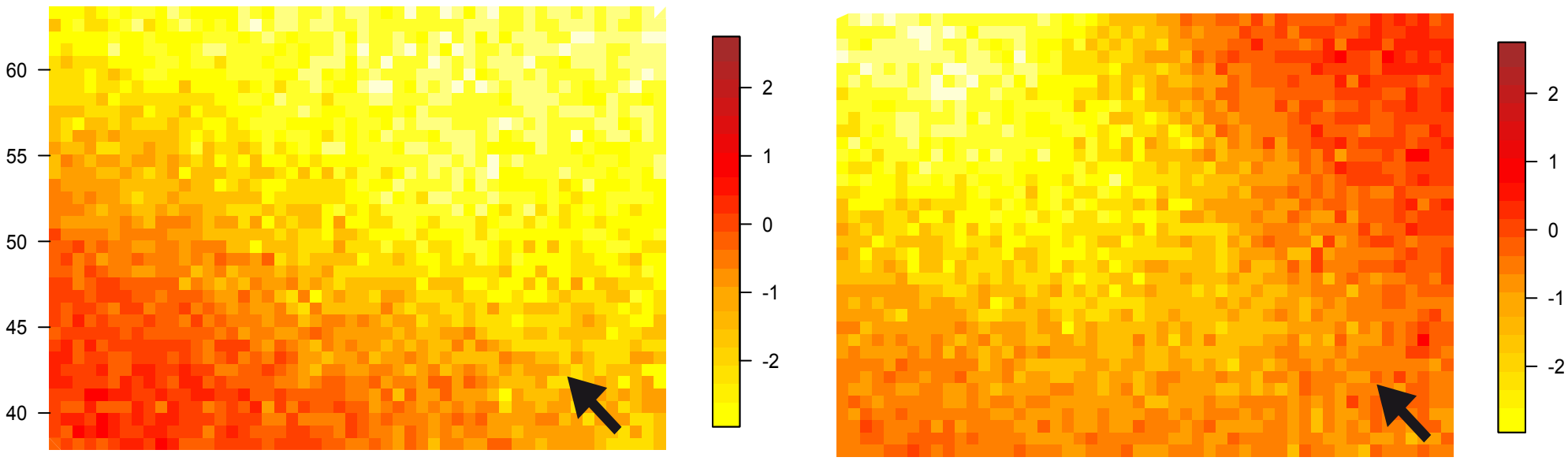
60
55
50
45
40
2
1
0
-1
-2
2
1
0
-1
-2

C

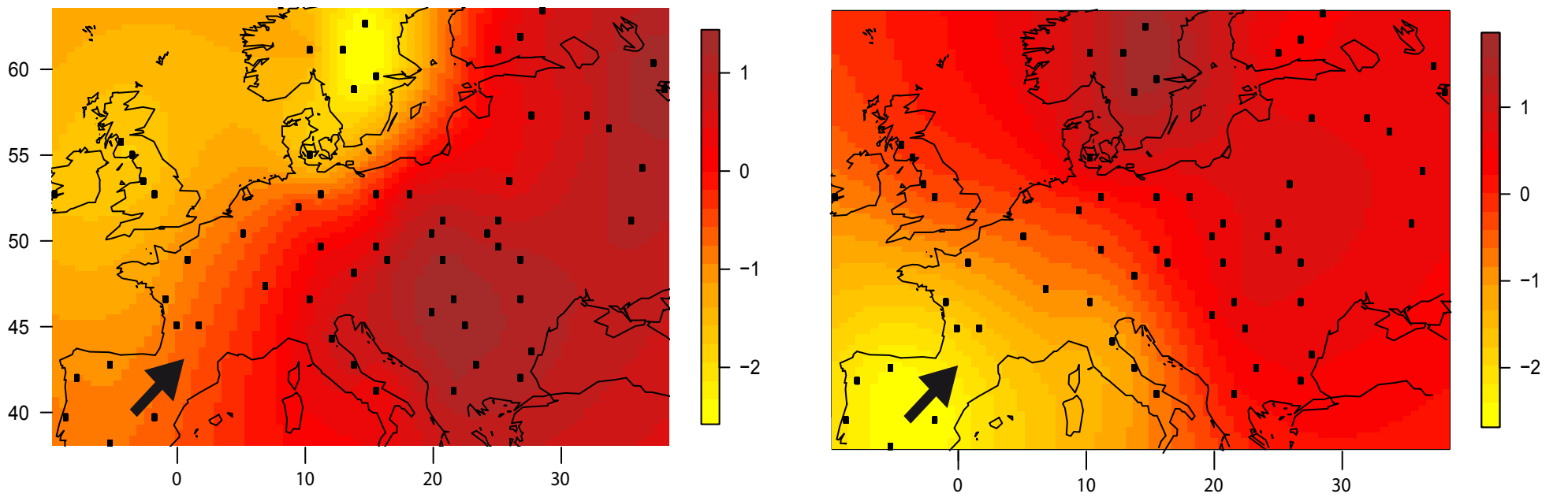
60
55
50
45
40
0
10
20
30
1
0
−1
−2
0
10
20
30
1
0
−1
−2

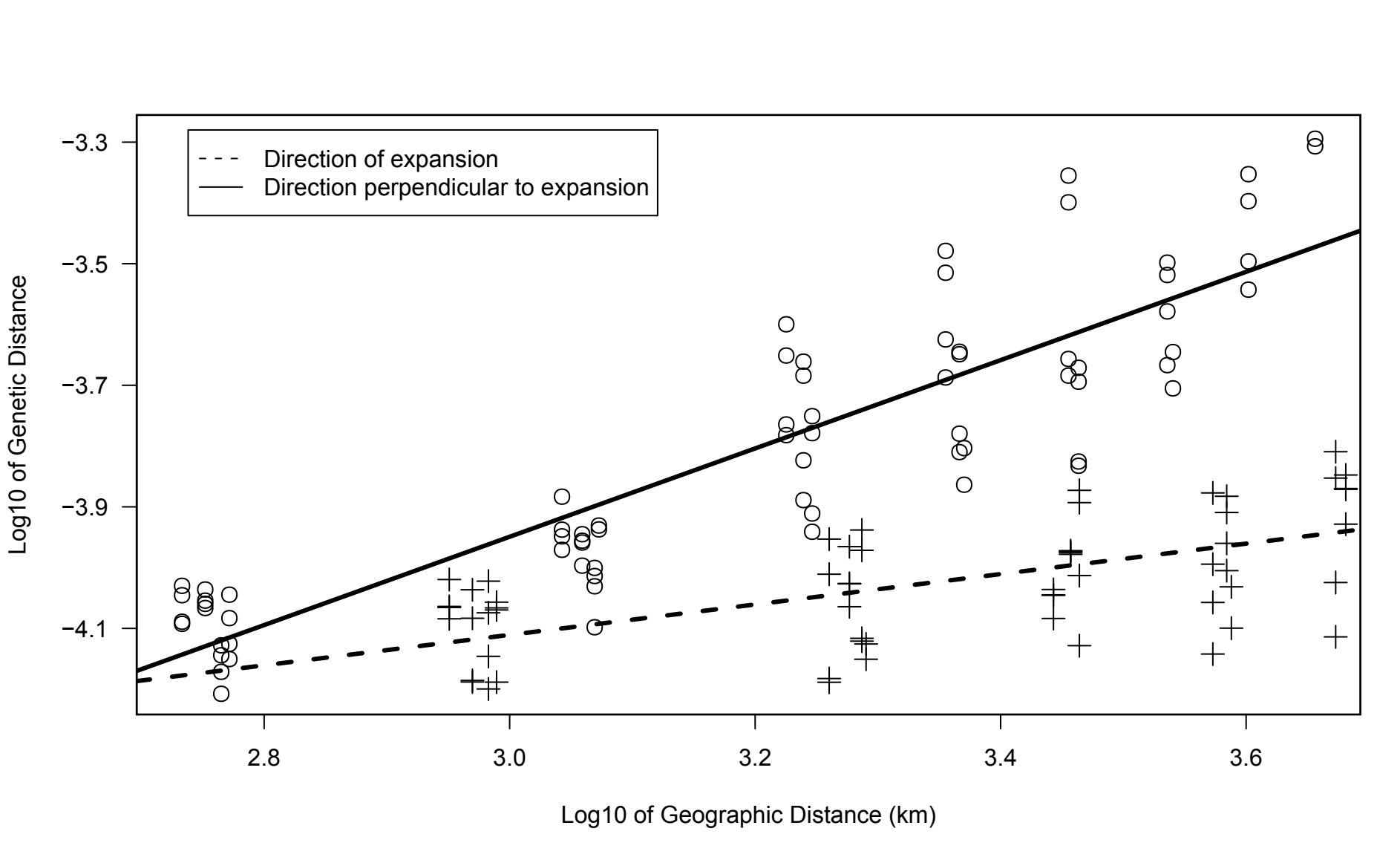
Direction of expansion
Direction perpendicular to expansion
−3.3
−3.5
−3.7
−3.9
−4.1
Log10 of Genetic Distance
2.8
3.0
3.2
3.4
3.6
Log10 of Geographic Distance (km)

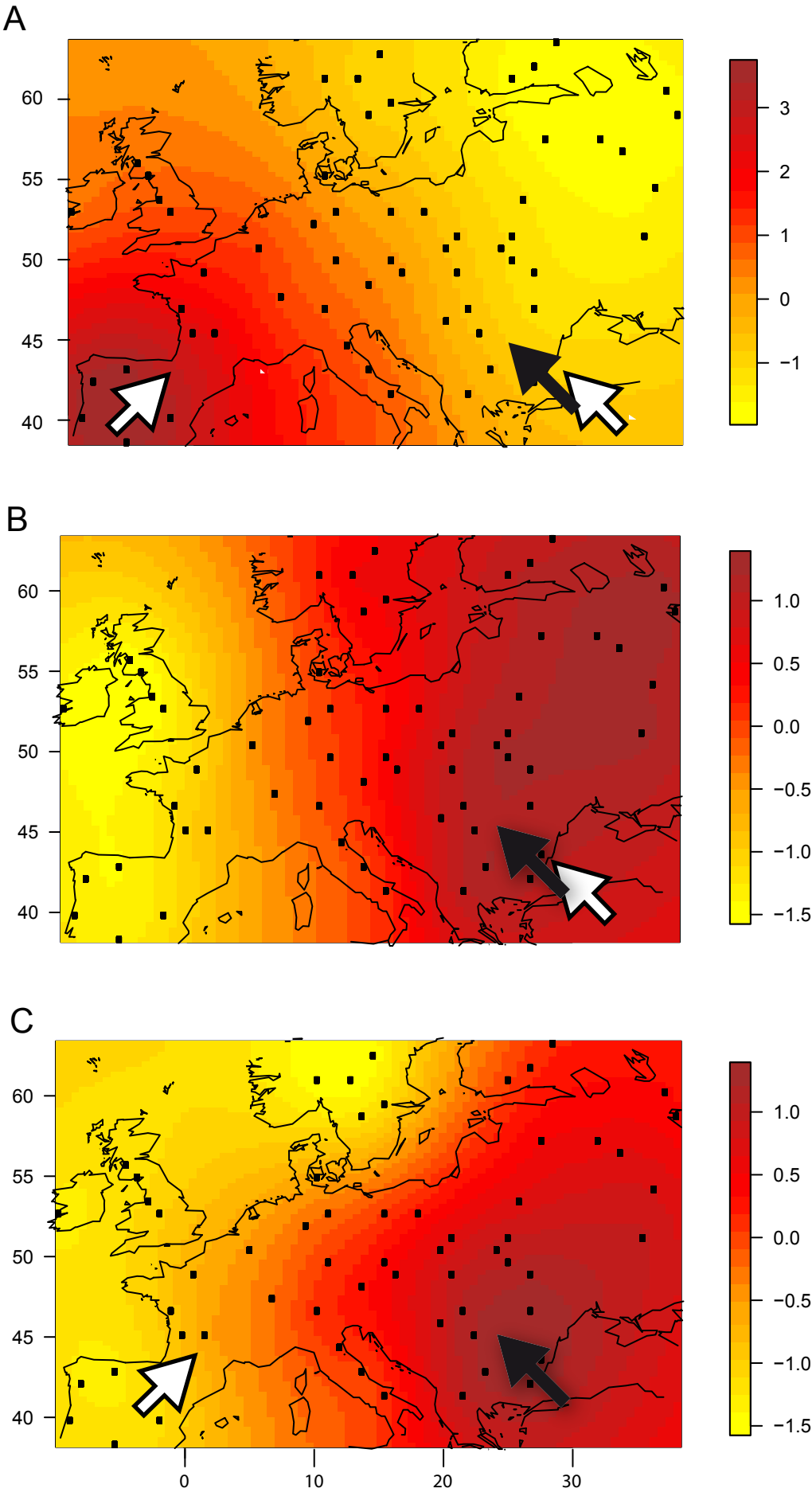
A
60
55
50
45
40
3
2
1
0
−1
B
60
55
50
45
40
1.0
0.5
0.0
−0.5
−1.0
−1.5
C
60
55
50
45
40
1.0
0.5
0.0
−0.5
−1.0
−1.5
0
10
20
30

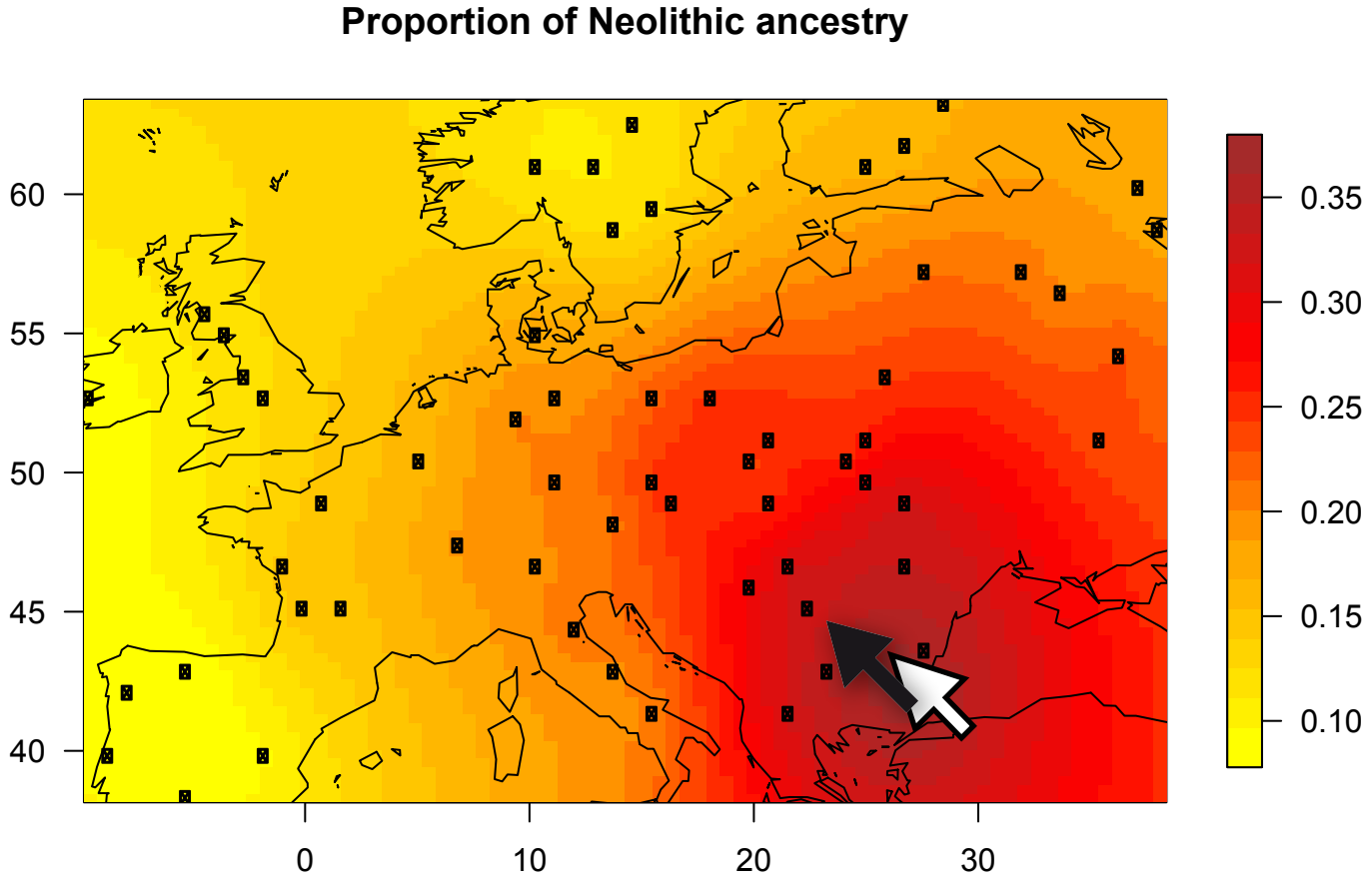
Proportion of Neolithic ancestry
60
55
50
45
40
0
10
20
30
0.35
0.30
0.25
0.20
0.15
0.10

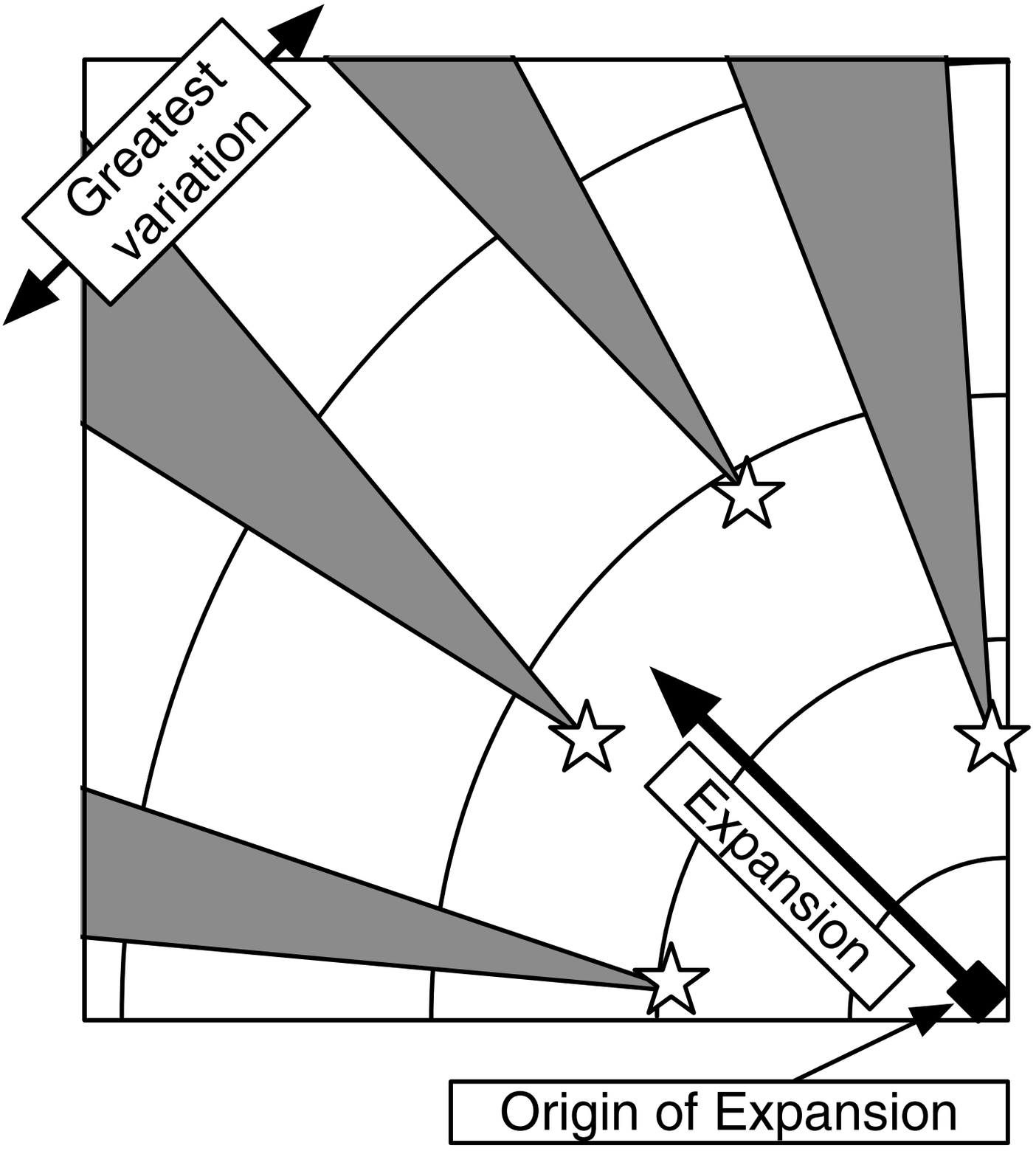

Locations of allele surfing events

Sectors where surfed allele is fixed

A

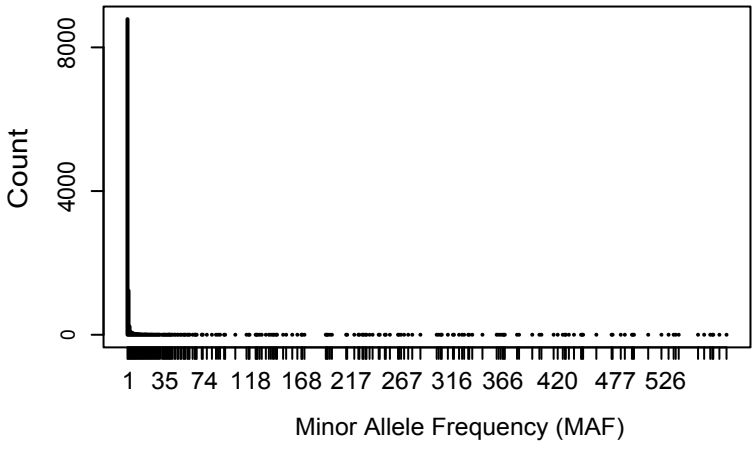
Count
0
4000
8000
1 35 74 118 168 217 267 316 366 420 477 526
Minor Allele Frequency (MAF)

B

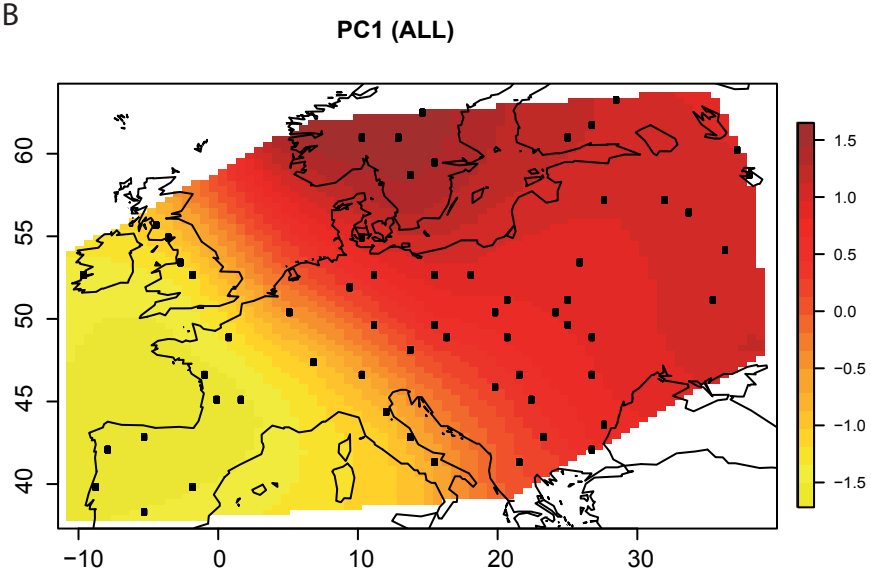
PC1 (ALL)
40
45
50
55
60
−10
0
10
20
30
1.5
1.0
0.5
0.0
−0.5
−1.0
−1.5

C

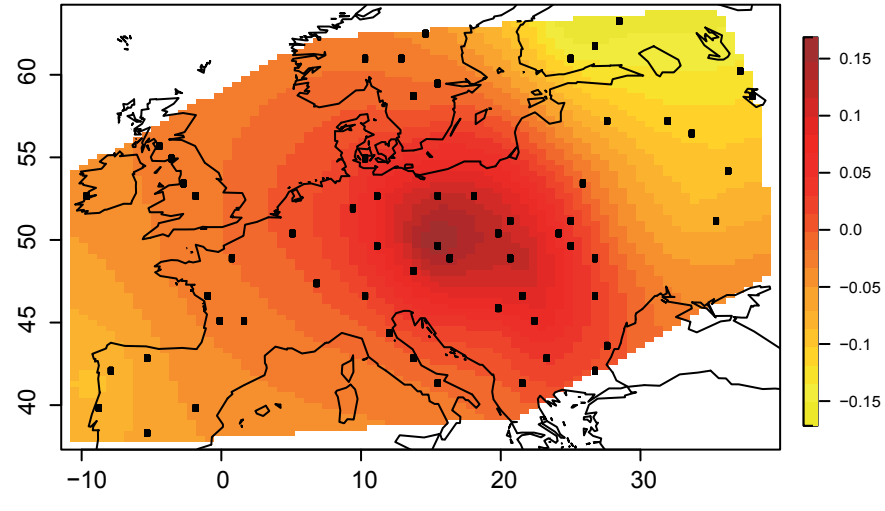
PC1 (MAF < 10)
40
45
50
55
60
−10
0
10
20
30
0.15
0.1
0.05
0.0
−0.05
−0.1
−0.15

D

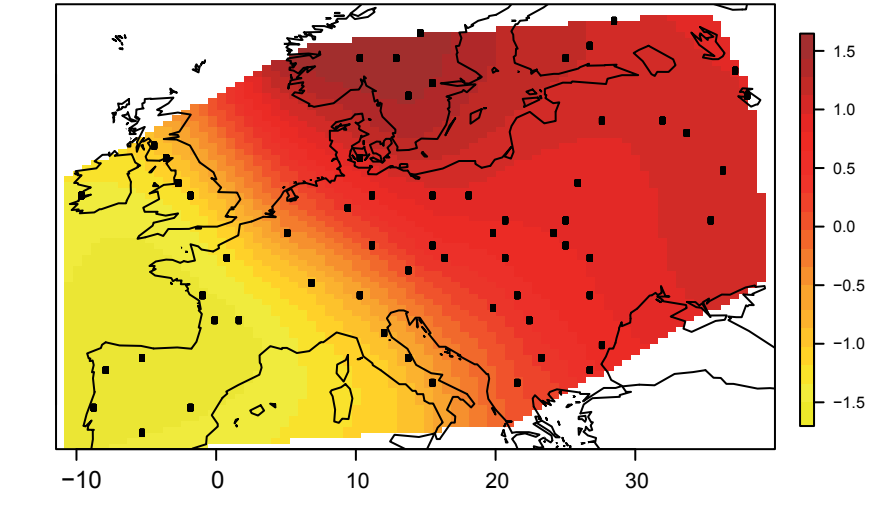
PC1 (MAF > 10)
−10
0
10
20
30
1.5
1.0
0.5
0.0
−0.5
−1.0
−1.5